Tissue and Cell 56 (2019) 60–70

Contents lists available at ScienceDirect

Tissue and Cell

journal homepage: www.elsevier.com/locate/tice

Multilineage potential research on pancreatic mesenchymal stem cells of bovine

Fan Gao[b,1], Yangnan Wu[a,1], Hebao Wen[c], Wanwan Zhu[a], Han Ren[c], Weijun Guan[a,*], Xiuzhi Tian[a,**]

[a] Institute of Animal Science of CAAS, Beijing 100193, China
[b] College of Human Movement Science, Harbin Sport University, Harbin, Heilongjiang, 150040, China
[c] Sports education and training learns, Mudanjiang normal university, Mudanjiang, Heilongjiang, 157012, China

ARTICLE INFO

Keywords:
Bovine
Mesenchymal stem cells
Pancreatic
Multiple differentiative potential

ABSTRACT

Stem cells are most likely to solve all three of diabetes's problems at once, but the previous studies have mostly focused on bone marrow mesenchymal stem cells (MSCs) and adipose tissue-derived MSCs, and few studies have been done on pancreatic MSCs. In this study, pancreatic was collected to isolate MSCs from bovine, and then their biological characteristics such as growth kinetics, surface antigen, and multilineage potential were examined. Pancreatic MSCs of bovine (B-PMSCs) could be cultured for 65 passages in vitro. Growth kinetics analyses indicated that B-PMSCs had a strong capacity for self-renewal in vitro and their proliferation capacity appeared to decrease by passaging. Surface antigen detection showed that B-PMSCs expressed CD29, CD44, CD73, CD90, CD106, CD166, Vimentin, Nestin and Insulin, but not expressed CD34 and CD45. Furthermore, B-PMSCs could be induced to differentiate into adipocytes, osteoblasts and smooth muscle cells as indicated by reverse transcription-polymerase chain reaction (RT-PCR) and immunofluorescence. Most importantly, insulin-secreting cell differentiation of B-PMSCs exhibited islet-like clusters and dithizone staining displayed scarlet, and the response of the islet-like clusters to glucose suggested that high concentration glucose (20 mM) could quickly and persistently stimulate insulin release, and from the 2.0 h of the stimulation, the insulin of 20 mM glucose group were significantly higher than the 5.5 mM group. The B-PMSCs were isolated successfully, and the cells owned powerful self-renewal ability and multiple differentiative potential. Therefore, the present study plays an important role by providing a PMSCs choice for cell therapy of diabetes and tissue engineering.

1. Introduction

Type 1 diabetes mellitus which caused by the destruction of pancreatic β-cells, can result in insulin dependency and hyperglycemia, therefore the patients need exogenous insulin injection. The traditional treatment is pancreas or pancreatic islet transplantation, which can promote endogenous insulin secretion. However, the shortage of donors and administration of immunosuppressive drug limit the application (Murai et al., 2017). In the recent years, on account of high availability of stem cells, an alternative therapeutic approach for type 1 diabetes mellitus was explored (Godfrey et al., 2012). Mesenchymal stem/stromal cells (MSCs) have been transplanted into human or animal models which were faced with heart disease, Crohn's disease, and stroke (Prockop and Olson, 2007; Uccelli and Prockop, 2010). Currently, insulin-producing β cells have been obtained from many different types of MSCs, such as bone marrow-derived MSCs (Phadnis et al., 2011), adipose tissue-derived MSCs (Okura et al., 2009), placenntal MSCs (Mathew and Bhonde, 2017) and Wharton's jelly-derived MSCs (Wang et al., 2011). Moreover, MSCs derived from human bone marrow (hBMMSCs) transplantation has been proved can preserve β cell functions in patients with type 1 diabetes mellitus (Carlsson et al., 2015). Some researches demonstrated that pancreatic MSCs may be more easily differentiated into β cells ccompared to other MSCs (Seeberger et al., 2006; Gopurappilly et al., 2013), and the increase of pancreatic β cells can increase insulin secretion. However, the lack of organ donors and the low yield of isolated islets limit the isolation and differentiation of these cells in vitro. Therefore, how to improve the production of donor resources and isolation of islets has become an

* Corresponding author at: Institute of Animal Science of CAAS, No. 2 Yuanmingyuan West Road, Haidian District, Beijing, China.
** Corresponding author.
E-mail addresses: guanweijun@caas.cn (W. Guan), tianxiuzhi@caas.cn (X. Tian).
[1] Co-first author.

https://doi.org/10.1016/j.tice.2018.12.001
Received 25 July 2018; Received in revised form 4 December 2018; Accepted 5 December 2018
Available online 06 December 2018
0040-8166/

Table 1
Primers used in the study.

Gene	Primers (5'-3')	Annealing temperature (°C)	Products (bp)
GAPDH	F: GGCAAGTTCAACGGCACAGTCA R: AAGTCCCTCCACGATGCCAAAG	60	364
CD29	F: GAAACTTGGTGGCATCGT R: CTCAGTGAAGCCCAGAGG	58	493
CD34	F: CCTCATCAGCTTTGCGACTT R: CCAGGAGCAAGGAGCACA	60	314
CD44	F: CGGAACATAGGGTTTGAGA R: GGTTGATGTCTTCTGGGTTA	56	301
CD45	F: CTACCCAACCTTCTACTCAA R: TTCACATCCAGGAGGTTC	56	221
CD73	F: CAATGGCACGATTACCTG R: GACCTTCAACTGCTGGATA	56	428
CD90	F: CACCACGCCCATTCAGTA R: TATTGGAGACGGAGGGATT	60	221
CD106	F: GTGAAGGCATTAACCAGG R: GCACAATAGAGCACGAGA	55	379
CD166	F: TATCAGGATGCTGGAAAC R: TAGCCAATAGACGACACC	55	498
Insulin	F: ACCCTGGTCGAGATGCTACT R: CAGTCAAGAGCAGGCTGACA	60	660
Nestin	F: AGAACCTCTGAGCCAAGTGC R: CATCAAGGGTGTCCTCCACC	60	428
Vimentin	F: AGCCAGTCCGTGCTACCG R: AACTCGGTGTTGATGGCGTC	62	338

urgent problem for scholars of all countries (Otonkoski et al., 2005).

Under defined conditions, mesenchymal stem cells have been shown to differentiate into many cells types, including osteoblasts, chondrocytes, adipocytes, endothelial cells, and smooth muscle cells (Marion and Mao, 2006; Williams and Hare, 2011), making them attractive candidates for cell-based disease therapies. However, the in vivo environment in which they are placed likely has a substantial impact in defining the fate and function of these cellsMost of the differentiation is drug induced, while the induction of smooth muscle cells is more commonly used in co-culture with endothelial cells (Lin and Lilly, 2014) or tissue extract. The recruitment and differentiation of vascular smooth muscle cells by endothelial cells is regulated by platelet-derived growth factor (PDGF), transforming growth factor-β (TGF-β), and Notch signaling (Gaengel et al., 2009).

As an important experimental animal, cattle play an important role in biomedical research. Firstly, fetal cattle are easy to acquired, and the quality of experimental materials is controllable. Therefore, it is convenient to carry out the research on bovine pancreas stem cells. More importantly, the study on bovine can avoid the ethical problems caused by the experiment of human fetus. Therefore, this study explored the isolation and culture of pancreatic MSCs of Chinese lusi cattle, and identificated the biological characteristics and the ability to differentiate into osteogenic, adipogenesis and smooth muscle cells, hoping to provide important experimental data for related experiments and the therapy of diabetes mellitus (Shapiro et al., 2006).

2. Materials and methods

2.1. Isolation and culture of the MSCs from pancreatic of bovine

All experimental animal protocols were approved and performed in accordance with the guidelines established by the Institutional Animal Care and Use Committee at the Chinese Academy of Agricultural Sciences. Miniature pigs were obtained from the Beijing miniature pig breeding base.

Bovine were collected after caesarean section (3–4 month) under sterile conditions. In this research 3 fetal bovine were used continually, which were transported to the laboratory within 4–8 h in an ice-box. The mesenteries of pancreatic were removed and then washed twice with phosphate-buffered saline (PBS) containing 1×10^4 IU/mL penicillin/streptomycin and then washed twice with low glucose Dulbecco's modified Eagle medium (L-DMEM; Gibco, Carslbad, CA, USA). Moreover, pancreatics were cut into 1mm3 tissue block, and incubated with 1% (w/v) type IV collagenase for 10 min and then incubated with 0.125% trypsase for another 10 min at 37 ℃ to dissociate the pancreatic cells. The digestion solution was filtered by 200 mesh screen, and then the cell suspension was centrifuged at 1200 rpm for 8 min at room temperature, the supernatant was discarded, and the pellet was re-suspended in complete medium consisting of DMEM/F12 (Gibco, Carslbad, CA, USA), 10% (v/v) fetal bovine serum (FBS) (Gibco, Carslbad, CA, USA), 10 ng/mL FGF-2 (PeproTech, Rocky Hill, TX, USA), 10 ng/mL epidermal growth factor (EGF) (PeproTech, Rocky Hill, TX, USA), 10 ng/mL LIF (PeproTech, Rocky Hill, TX, USA), 2 mM Lglutamine, and 1×10^4 IU/mL penicillin/streptomycin. Nucleated cells (1×10^6/cm^2) were seeded on culture plates in complete medium. The cells were incubated at 37 ℃ in a humidified atmosphere containing 5% CO_2. At 2 days after seeding, the cells were washed twice with PBS to remove non-adherent cells.

2.2. Immunofluorescence of B-PMSCs surface markers

Firstly, the B-PMSCs were fixed in 4% (w/v) paraformaldehyde for 30 min and then washed thrice using PBS. Secondly, the B-PMSCs were permeabilized by incubation in 0.2% (v/v) Triton X-100 for 20 min and

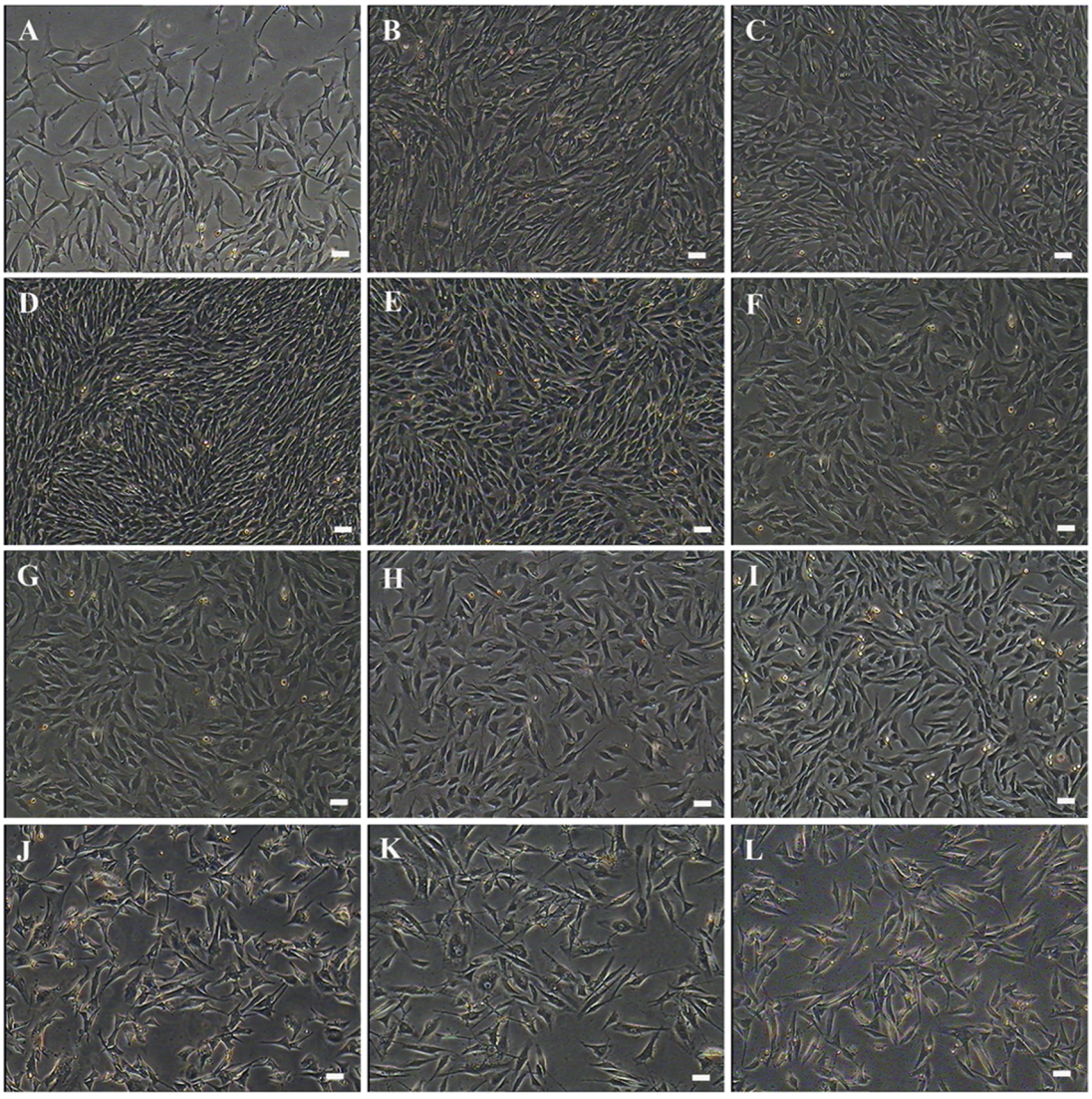

Fig. 1. Morphology of primary cultured and subcultured B-PMSCs. **A–L** are representative cellular morphologies of passage 0, 1, 2, 8, 5, 10, 20, 30, 40, 50, 60, 64 and 65 B-PMSCs, respectively (scale bar = 100 μm).

then washed thrice using PBS. Next the cells were blocked in 10% goat serum (Zhongshan Golden bridge, Beijing, China) for 30 min and then incubated in 10% (w/v) goat serum containing the following antibodies: rabbit anti-bovine CD44, CD73, Fibronectin, Nestin and Vimentin (1 : 100) (Abcam, Cambridge, MA, USA) for overnight. Finally, the cells were washed thrice using PBS and incubated in PBS containing a fluorescein isothiocyanate-conjugated mouse anti-rabbit secondary antibody (Santa Cruz Biotechnology, Santa Cruz, CA, USA) for 1 h at 37 ℃ keeping in dark. After incubation, the cells were washed thrice using PBS and then counterstained with DAPI (Sigma-Aldrich, St Louis, MO, USA) and examined under a Nikon TE-2000-E confocal microscope.

2.3. RT-PCR analysis

Total RNA was extracted using Trizol reagent (Invitrogen, Carlsbad, CA, USA). RNA concentrations were measured by absorbance at 260 nm with a spectrophotometer and 2 μg of DNase I-treated RNA of each sample served as a template for a one-step reverse transcription-polymerase chain reaction (RT-PCR) system (Takara, Dalian, Liaoning Province, China) and then amplified by PCR using the specific primers listed in Table 1. The primers were designed with Primer Premier 5.0 software (Premier Biosoft, Palo Alto, CA, USA) and primers were spanned an exon–intron boundary. The PCR products were visualized with ethidium bromide on a 2% agarose electrophoresis.

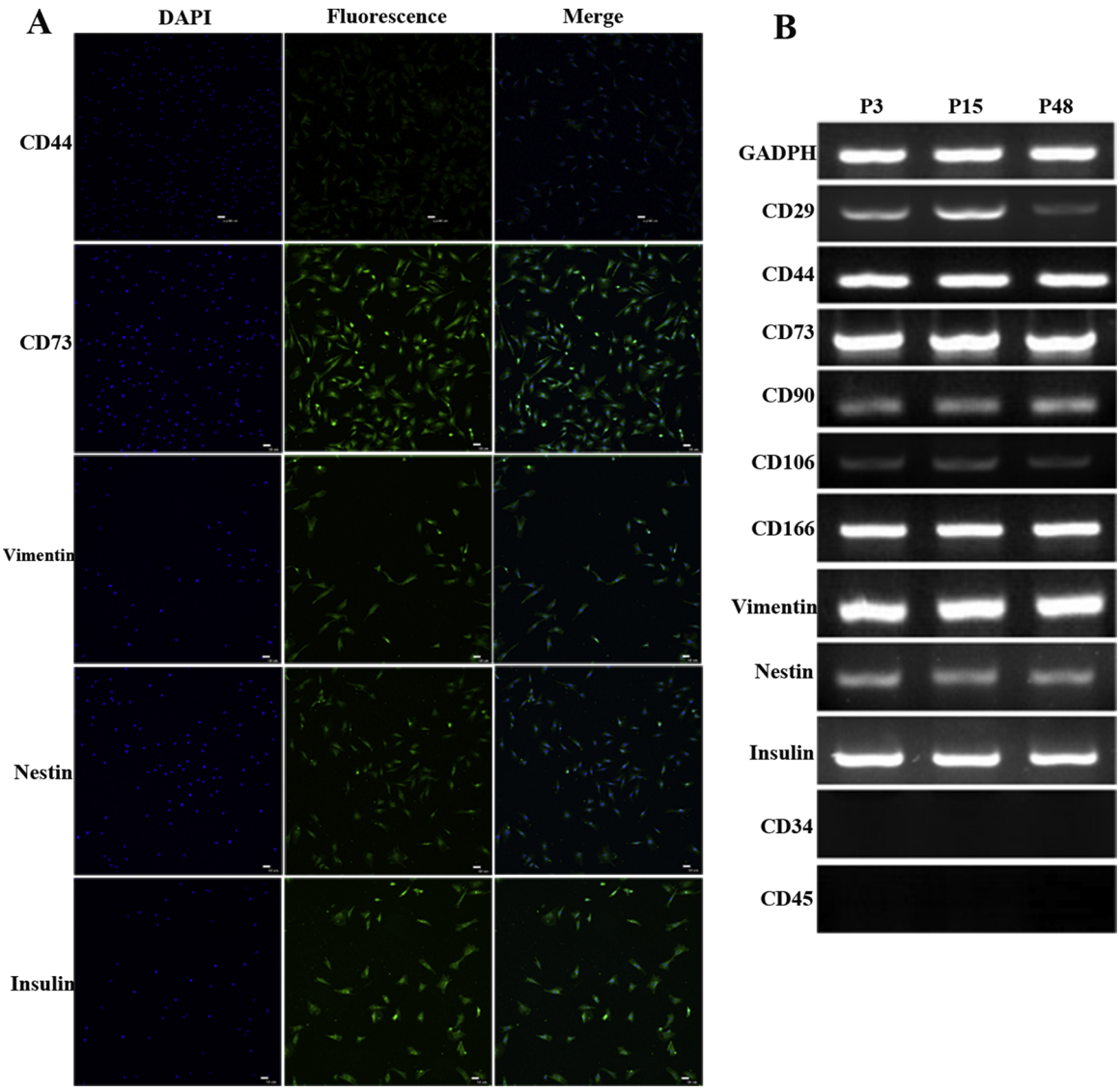

Fig. 2. Characteristics of B-PMSCs surface antigens at different passages. **A** Immunofluorescence showing CD44, CD73, Vimentin, Nestin and Insulin positive cells (scale bar = 100 μm). **B** RT-PCR analysis showed that B-PMSCs at passages 3, 15, 48 express CD29, CD44, CD73, CD90, CD106, CD166, Vimentin, Nestin and Insulin. GAPDH served as the internal control.

2.4. Growth Kinetics and survival rate of cryopreservation

The B-PMSCs at passages 3, 15 and 48 were used to analyze the growth kinetics of B-PMSCs. The cells were harvested and seeded in 24-well culture plates at a density of 1×10^4 cells/well. The cells from three random wells were counted each day for 8 days. Growth curves were plotted according to the mean values, and the PDT calculated by the growth curve. PDT = $(t\text{-}t_0)\ lg_2/(lgNt\text{-}lgN_0)$. where t_0 = starting time of culture; t = termination time of culture; N_0 = initial cell number of culture; Nt = ultimate cell number of culture. The B-PMSCs at passages 3, 15 and 48 were used to analyze the survival rate of cryopreservation by counting the percentage before and after cryopreservation.

2.5. Single cell cloning

The B-PMSCs at passages 3, 15 and 48 were digested using 0.25% trysin/EDTA and diluted to produce single-cell suspention, and then seeded in 60-mm plates at a density of 20 cell/cm^2. After 14 days, the B-PMSCs were stained with Giemsa and colony forming efficiency (CFE) was counted and the cloning efficiencies were calculated as: CFE = colony forming unit number/starting cell number ×100% (Gao et al., 2012).

2.6. Cell cycle examination

The B-PMSCs at passages 3, 15 and 48 were digested using 0.25% trysin/EDTA and centrifuged to collect cells, and then washed the cells

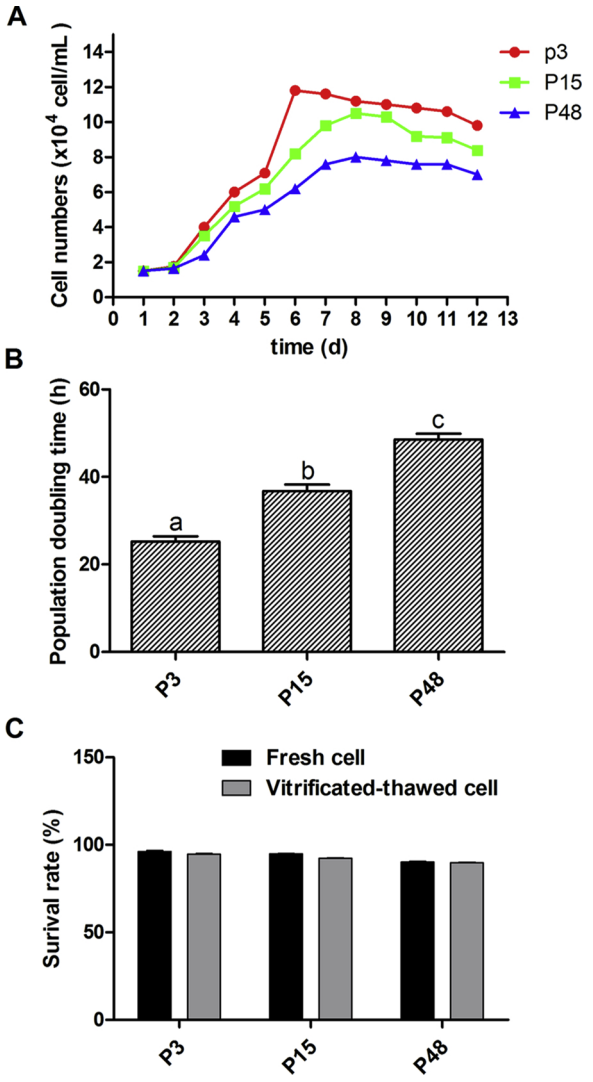

Fig. 3. Growth kinetics and survival rate of cryopreservation assay. **A** The growth curves of P3, P15, and P48 B-PMSCs were all typically sigmoidal, with cell density reflected by the vertical axis. The growth curve consisted of a latent phase, a logarithmic phase, and a plateau phase. **B** The PDT of B-PMSCs was significantly different between passages. **C** The survival rate of cryopreservation assay showed no difference ($P < 0.05$).

thrice using PBS. Next, added the precooled 70% ethanol for fixating the single-cell for one night at 4 ℃. Finally, 1000 rpm, 10 min centrifugation to wash the cells and then stain the cells using PI at 4 ℃ for 30 min, and detect the cells on the flow cytometry machine. Every generation cells was detected three times and the total number of each sample must be greater than 1×10^4 cells/well.

2.7. Osteogenic differentiation of B-PMSCs

The P3 B-PMSCs were used for osteogenic differentiation. The cells were grown to approximately 60% confluence and then cultured in osteogenic differentiation medium consisting of DMEM/F12, 10% FBS, 0.1 mM dexamethasone, 10 mM β-glycerophosphate, and 50 mg/L vitamin C. Control cells were cultured in complete medium without any inducers. The medium was changed every 2 days. The cells were cultured for 2 weeks until significant calcium deposits were observed. Then, the cells were washed twice, and then fixed in 4% paraformaldehyde, and finally stained with Alizarin Red S that specifically stains calcified deposits in the extracellular matrix. Additionally, the expression of osteoblast-specific genes collogen-1 (COL 1) and osteopontin (OPN) was analyzed by RT-PCR.

2.8. Adipogenic differentiation of B-PMSCs

The P3 B-PMSCs were used for adipogenic differentiation. The cells were grown to approximately 60% confluence and then cultured in adipogenic differentiation medium consisting of DMEM/F12, 10% FBS, 1 mM dexamethasone, 0.5 mM isobutyl-methylxanthine, and 10 mg/L insulin. Control cells were cultured in complete medium. The medium was changed every 2 days. The cells were cultured for 2 weeks until significant lipid droplets were observed in the cytoplasm. The cells were then washed, fixed in 4% paraformaldehyde, and stained with Oil Red O (Sigma) to assess intracellular lipid accumulation. Additionally, the expression of adipogenic-specific genes peroxisome proliferator-activated receptor-γ (PPAR-γ) and lipoprotein lipase (LPL) was analyzed by RT-PCR.

2.9. Smooth muscle cell differentiation of B-PMSCs

The P3 B-PMSCs were used for smooth muscle cell differentiation. Cells were grown to 60% confluence and then cultured in the induction medium consisting of DMEM/F12, 5% equine serum, 30 ng/mL vascular endothelial growth factor, and 10 ng/mL FGF-2. Control cells were cultured in complete medium. The medium was changed every 2 days. After 12 days, the cells were harvested and α-SMA, calponin-1 and SM-MHC were analyzed by immunofluorescence.

2.10. Insulin-secreting cell differentiation of B-PMSCs and it's response to glucose

The P3 B-PMSCs were used for insulin-secreting cell differentiation. Cells were grown to 60% confluence and then cultured in the induction medium consisting of DMEM/F12, 10% FBS and 10^{-6} mol/L retinoic acid, 5 ng/mL HGF, 10 ng/mL EGF for 21 days. Dithizone (DTZ, Sigma-Aldrich, St Louis, MO, USA) were used to assess the differentiation. And then the islet-like cells were cultured in 5.5 mM and 20 mM glucose stimulation medium (DMEM/F12, 10% FBS and 5.5 mmol/Lor 20 mmol/L glucose) seperately, and collecting the culture medium at 0 h, 0.5 h, 1.0 h, 2.0 h, 4.0 h and 8.0 h, storage at -20℃ for insulin assay. Radioimmunoassay was used to determine the insulin of the culture medium.

2.11. Statistical analysis

The data are presented as the means ± SEM. The data were analyzed with the one-way analysis of variance (ANOVA) followed by Tukey method using the SPSS 20.0 statistical software (SPSS Inc., Chicago, IL, USA). Statistical significance was set at $P < 0.05$.

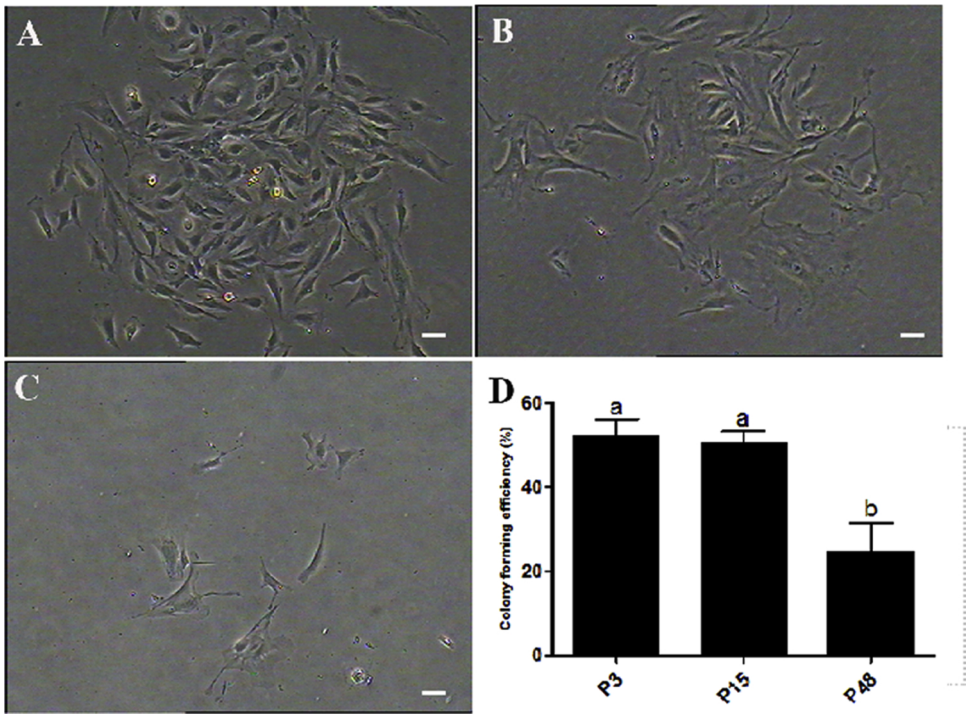

Fig. 4. Colony forming assay. **A–C** displays the representative colony of P3, P15 and P48 B-PMSCs, respectively. **D** Colony forming efficiency. The B-PMSCs at passages 3 and 15 showed significantly difference from the B-PMSCs at passage 48 ($P < 0.05$). (scale bar = 100 μm).

3. Results

3.1. Isolation, culture and morphological observations of B-PMSCs

The primary cells isolated from bovine pancreas were mixed with a lot of blood cells and gland cells. Twenty-four hour later after isolation, the primary cells began to adhere to the well surface, some cells exhibited polygonal and long fusiform morphology, and others aggregated and grew into islet-like clumps cells. At the 10th day of culture, the cell confluence reached about 80%, and then handed from generation to generation.The third generation cells were basically purified and all cells showed the same mpolygonal shape orphology. As the generation increasing, the cell volume began to increase, and some cells showed long fusiform, but still maintained strong growth ability. The cells were cultured to passage 65 until the 240th day in vitro and displayed a representative senescent appearance including blebbing and karyopyknosis in most cells (Fig. 1).

3.2. Surface marker detection of B-PMSCs

The surface markers of B-PMSCs were detected on P3, P15, P48 cells by immunofluorescence and RT-PCR. Immunofluorescence staining showed that the B-PMSCs were positive for CD44, CD73, Vimentin, Nestin and Insulin (Fig. 2). RT-PCR also indicated that the B-PMSCs expressed CD29, CD44, CD73, CD90, CD106, CD166, Vimentin, Nestin and Insulin, but not expressed CD34 and CD45. Densitometry indicated that the expression of CD73 and Vimentin was higher than that of the other genes (Fig. 2).

3.3. Growth kinetics and surival rate

The growth kinetics of B-PMSCs at P3, P15, P48 passages was calculated by growth curves that were all typically sigmoidal. The B-PMSCs at P3, P15, P48 passages entered the logarithmic phase after 1 day culture, followed by the plateau phase after 6 days culture (Fig. 3A). The population doubling time (PDT) of passage 3, 15 and 48 were significantly different (25.2, 36.8, and 48.6 h for passage 3, 15 and 48 respectively), which indicated that with the passages increasing the B-PMSCs had a high proliferation potential in vitro, but the proliferation rate decreased (Fig. 3B). Furthermore, the survival rates before and after cryopreservation of the B-PMSCs at passages 3 and 15 were significantly higher than that of the passage 48 (Fig. 3C), which indicated that in the same process of cryopreservation, the capacity of resistance to freezing of the high-generation cells is weaker than that of the low-generation cells.

3.4. Single cell cloning

After 14 days culture, the colony forming capacity of the B-PMSCs at passages 3, 15 and 48 was stained by Giemsa. The colony forming efficiency rates were 52.2% ± 3.97%, 50.3% ± 3.02% and 24.7% ± 6.7% respectively. These results demonstrated that the cultured B-PMSCs at passages 3, 15 and 48 owned potent self-renewal capacity (Fig. 4).

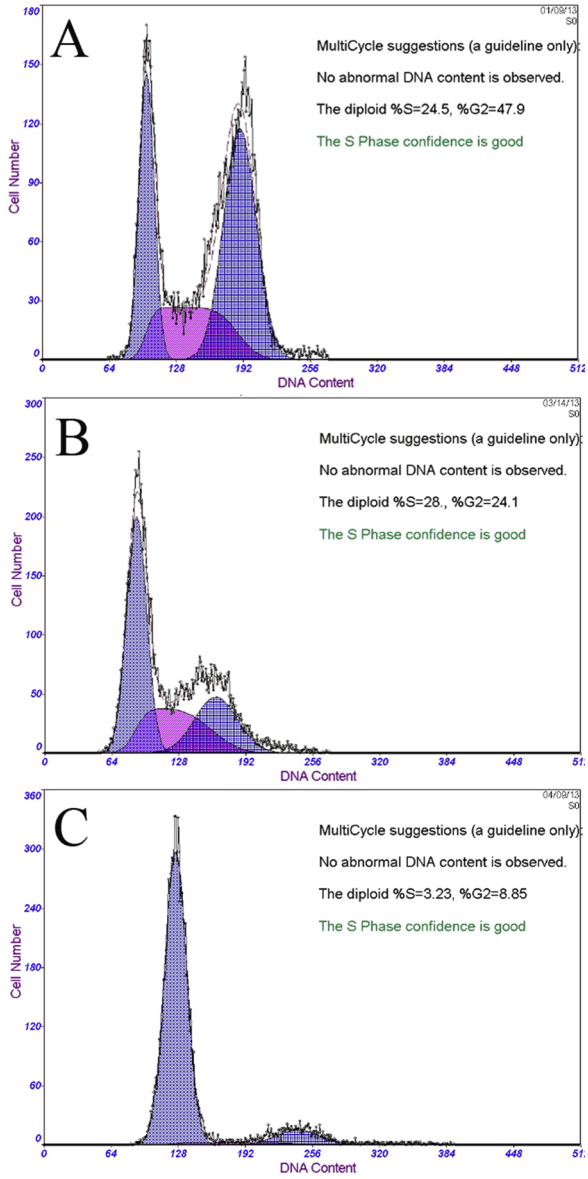

Fig. 5. Cell cycle examination assay. **A–C** represents the cell cycle of P3, P15 and P48 B-PMSCs, respectively.The B-PMSCs at passages 3and 15 showed significantly difference from the B-PMSCs at passage 48.

3.5. Cell cycle examination

The results of flow cytometry showed that most of the cells at passages 3, 15 and 48 were at rest phase (G0/G1). As the generations going up, cells at rest phase gradually increased, while cells in the division phase showed a weakening trend. The B-PMSCs at passages 3 and 15 showed significantly difference from the B-PMSCs at passage 48 (Fig. 5).

3.6. Osteogenic differentiation of B-PMSCs

After incubation in osteogenic induction medium, the cell proliferation rate was significantly accelerated, and after 2 days, the cells completely confluent and the volume started to increase, the shape became irregular, and the dense growth of the cell made it unable to maintain the spiral shape. After induction for 8–12 days, the B-PMSCs exhibited obvious morphological changes, there were many nodular structure could be seen in the center and the edge had strong refractive power under microscope. The cells changed from polygon to tridimensional and then aggregated and formed mineralized nodules. Control cells cultured in complete medium showed no change in morphology. Furthermore, the nodules were positive for Alizarin Red staining and increased and grew in size during culture (Fig. 6B), but the control cell were negative by Alizarin Red staining. Osteogenic differentiation of the B-PMSCs was also analyzed by RT-PCR, and the results displayed that the induced cells expressed specific genes collage type I (Coll I) and OPN (Fig. 6E).

3.7. Adipogenic differentiation of B-PMSCs

After incubation in adipogenic medium, the cell morphology did not change significantly. At the fifth day, the cells are completely fused and some cells morphology began to change, the appearance of long spindle cells gradually became round and the volume became larger, the cells showed multipole protuberances and enhanced refractive ability. Subsequently, small lipid droplets appeared in the cell. With the increase of induction time, the number and volume of lipid droplets gradually increased, and some lipid droplets began to condense into large lipid droplets. Oil Red O staining demonstrated that the induced cells were positive and had an adipogenic ability while the control cells cultured in complete medium were negative (Fig. 7A–C). Furthermore, RT-PCR revealed that the B-PMSCs expressed the adipocyte specific genes LPL and PPAR-γ, while the control cells didn't express this two genes (Fig. 7D).

3.8. Smooth muscle cell differentiation of B-PMSCs

After incubation in smooth muscle cell medium for 14 days, the B-PMSCs exhibited obvious morphological variation. The cells changed from polygon to fusiform smooth muscle. Control cells cultured in complete medium showed no change in morphology. Furthermore, smooth muscle cells merged to form the peak valley pattern, and expressed specific protein markers α-SMA, calponin-1 and SM-MHC (Fig. 8).

3.9. Insulin-secreting cell differentiation of B-PMSCs and it's response to glucose

After incubation in insulin-secreting cell medium for 10 days, the B-PMSCs exhibited islet-like clusters firstly, and until at 21 day there were more obvious islet-like clusters, Dithizone staining displayed scarlet (Fig. 9). Moreover, the detection of insulin secret response to glucose indicated that the ability of insulin secret of the induced islet-like clusters depended on glucose concentration and time (Fig. 10). High concentration glucose (20 mM) could quickly and persistently stimulate insulin release. And from the 2.0 h of the stimulation, the insulin of 20 mM glucose group were significantly higher than the 5.5 mM group (Fig. 10).

4. Discussion

As is known to all, diabetes brings 3 main problems: 1) vascular injury; 2) islet injury; 3) blood glucose fluctuation, and in which insulin

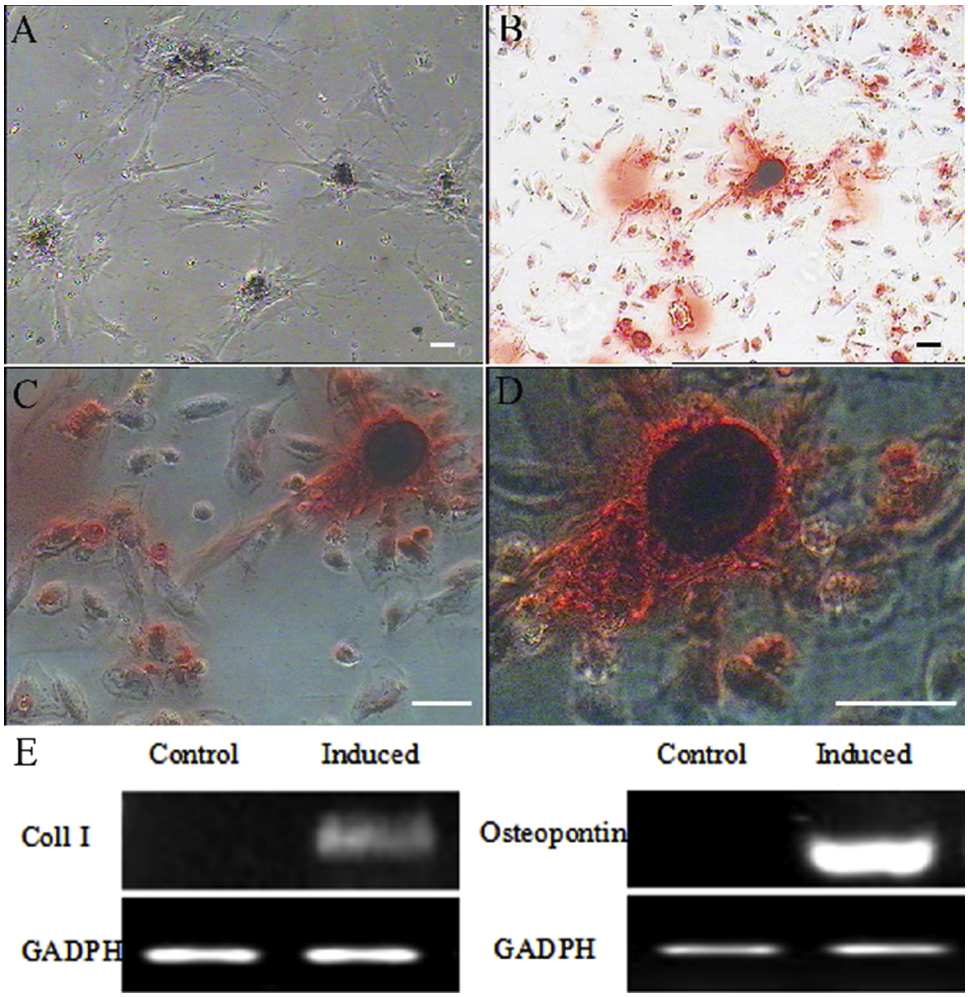

Fig. 6. Osteogenic differentiation of B-PMSCs. **A** Control cells (40×); **B** After induction in osteogenic medium for 14 days, the cells changed from fusiform to triangular in shape and were positive for alizarin red staining (40×); **C** Alizarin red staining (100×); **D** Alizarin red staining (200×); **E** After induction for 14 days, RT-PCR revealed the expression of osteoblast-specific genes Coll I and Osteopontin (OPN) in the induced group, whereas these genes were not expressed in the control group. GAPDH served as the internal control. (scale bar = 100 μm) (For interpretation of the references to colour in this figure legend, the reader is referred to the web version of this article).

can only reluctantly solve the blood glucose fluctuation. Only stem cells are most likely to solve all three of diabetes's problems at once. Stem cell and islet transplantation directly solve the immune intervention and islet function recovery, striving to reshape the physiological insulin secretion in the body and reignite the new hope of treating type 1 diabetes. MSCs are capable of microenvironment modification of injured tissues contributing to tissue regeneration and repair through anti-inflammatory and anti-apoptotic mediators (Yeung et al., 2012). The previous studies have focused on bone marrow mesenchymal stem cells (Phadnis et al., 2011; Carlsson et al., 2015) and adipose tissue-derived MSCs (Okura et al., 2009), and have demonstrated that MSCs transplantation decreased blood glucose levels and enhance the regeneration of pancreatic islet of diabetic animals (Boumaza et al., 2009).

In this study, bovine pancreatic mesenchymal stem cells (B-PMSCs) were successfully isolated from 3 to 4 month old fetal bovine. The B-PMSCs could be cultured for 65 passages. The results of growth kinetics indicated that the B-PMSCs at 48 passages still had a very high proliferative ability. Moreover, the B-PMSCs could be induced to differentiate into osteoblasts, adipocytes and smooth muscle cells. Therefore, the acquired B-PMSCs own powerful self-renewal ability and multipotential differentiation.

As we know that the surface markers of MSCs from different sources are usually different. Generally, bone marrow mesenchymal stem cells are positive for SH3, CD44, CD71, CD90, CD106, Vimentin and Fibronectin, but negative for CD45, CD34, CD31 and CD14 (Silva et al., 2012). Metanephric MSCs are positive for CD29, CD44, CD71, CD73, CD166, Pax2, Vimentin and Fibronectin et al., while negative for CD34, CD31 and CD45 (De Schauwer et al., 2011; Wen et al., 2018). In this study, the immunofluorescence staining suggested that B-PMSCs were positive for CD44, CD73, Vimentin, Nestin and Insulin, while RT-PCR results indicated that the B-PMSCs expressed CD29, CD44, CD73, CD90, CD106, CD166, Vimentin, Nestin and Insulin, but not expressed CD34 and CD45. Furthermore, densitometry indicated that the expression of CD73 and Vimentin was higher than that of the other genes. The results revealed the established cell line expressed the markers of MSCs which was in accordance with Bai et al (Bai et al., 2015), and no obvious differences were found among passages 3, 15 and 48.

Cell growth curve, surival rate of cryopreservation and colony forming ability were investigated to declare the proliferation and self-

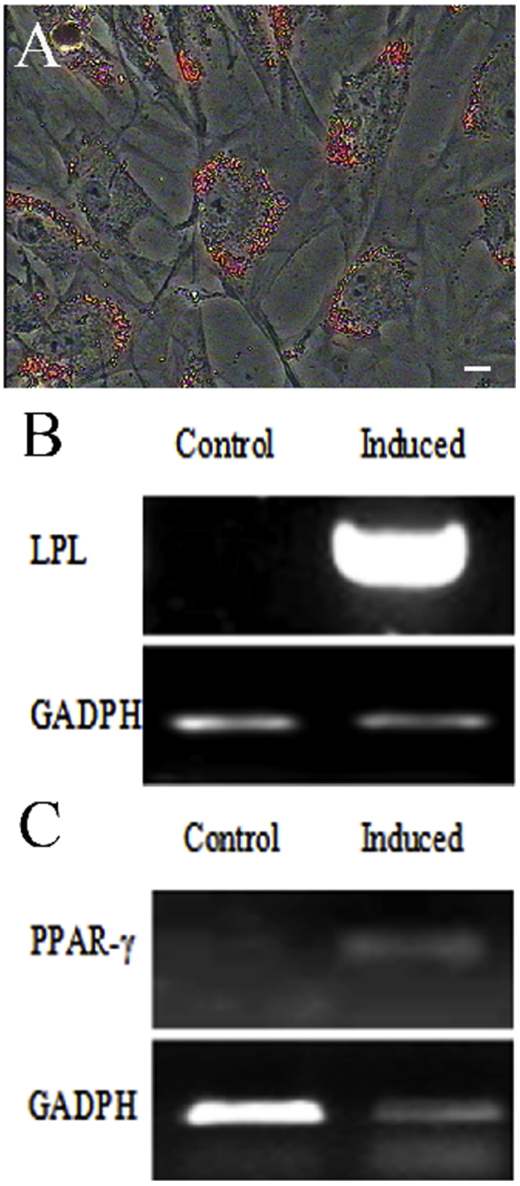

Fig. 7. Adipogenic differentiation of B-PMSCs. **A–C** Induced cells were Oil Red O positive (200×); D RT-PCR analysis of adipocyte-specific genes LPL and PPAR-γ. (scale bar = 100 μm) (For interpretation of the references to colour in this figure legend, the reader is referred to the web version of this article).

renewal ability of the B-PMSCs. The growth curves of the B-PMSCs at passages 3, 15 and 48 all appeared typically sigmoidal shape which were composed of lag, logarithmic and plateau phases and conformed with the reported research (Gao et al., 2014; Ma et al., 2016). As the generations going on, the proliferation and self-renewal ability of the B-PMSCs declined and the PDT was prolonged from 25.2 h to 48.6 h. The survival rate before and after cryopreservation of the B-PMSCs at passages 3 and 15 was higher than that of the passage 48 suggested that the anti-freeze ability of high generation cells was better than the low generation cells. Moreover, the clonal efficiency demonstrated powerful self-renewal potential of the B-PMSCs which was consistent with the result of cell cycle examination.

Plenty of studies have demonstrated that MSCs are able to differentiate into adipogenic, osteogenic, myogenic, chondrogenic and neurogenic cell types, which suggests that MSCs have wide application value in clinic (Damia et al., 2018; Mendes et al., 2018; Badimon et al., 2015). Importantly, stem cell-based kidney regeneration could help in reducing the incidence and severity of kidney disease (Jiao et al., 2011; Sagrinati et al., 2008; Little, 2006). In the current work, osteogenic differentiation of the B-PMSCs resulted in the spindle-shaped, polygonal or triangular cells changing into diamond-shaped osteoblasts, and accompanied by the formation and sediment of minerals in the extracellular matrix of the differentiated cells. And Alizarin Red staining was positive. Moreover, RT-PCR analyses demonstrated that the differentiated cells expressed the osteogenic specific genes collagen type I and OPN which was consistent with the previous studies (Bai et al., 2015; Gao et al., 2014). Furthermore, the B-PMSCs also could be induced to adipogenic cells and resulted in oblate cells with many lipid droplets were present in the cells by addition of insulin and isobutylmethylxanthine. The results also showed that the number of droplets increased as the induction time going on, and many small lipid droplets would assembled to form larger lipid droplets. The Oil Red O staining suggested that the induced cells were positive and had adipogenic ability. RT-PCR analyses showed that the differentiated cells expressed adipogenic-specific genes PPAR-γ and LPL. In addition, the B-PMSCs also could be induced to differentiated to smooth muscle cells by expressing the smooth muscle cell specific protein markers α-SMA, calponin-1 and SM-MHC. Moreover, insulin-secreting cell differentiation of B-PMSCs exhibited islet-like clusters and dithizone staining displayed scarlet, which was consistant with the induction of Tibetan Mastiff pancreatic progenitor cells (He et al., 2018). Most importantly, the result of insulin secret of the islet-like clusters response to glucose suggested that high concentration glucose (20 mM) could quickly and persistently stimulate insulin release. And from the 2.0 h of the stimulation, the insulin of 20 mM glucose group were significantly higher than the 5.5 mM group.

5. Conclusion

In this study, all the results demonstrated that the B-PMSCs isolated from Bovine were pancreatic mesenchymal stem cells, owning potent self-renewal ability and differential potential. The successful acquisition of pancreatic mesenchymal stem cells will provide a new type stem cell source and technical guidance for stem cell transplantation for diabetes disease, and has important effect on the potential application of B-PMSCs for regenerative therapies of human diseases, especially pancreatic related diseases. Moreover, the present study provides valuable information for the preservation of genetic resources and the study of cell biology and genomics.

Conflict of interest

The authors declare that they have no conflict of interest.

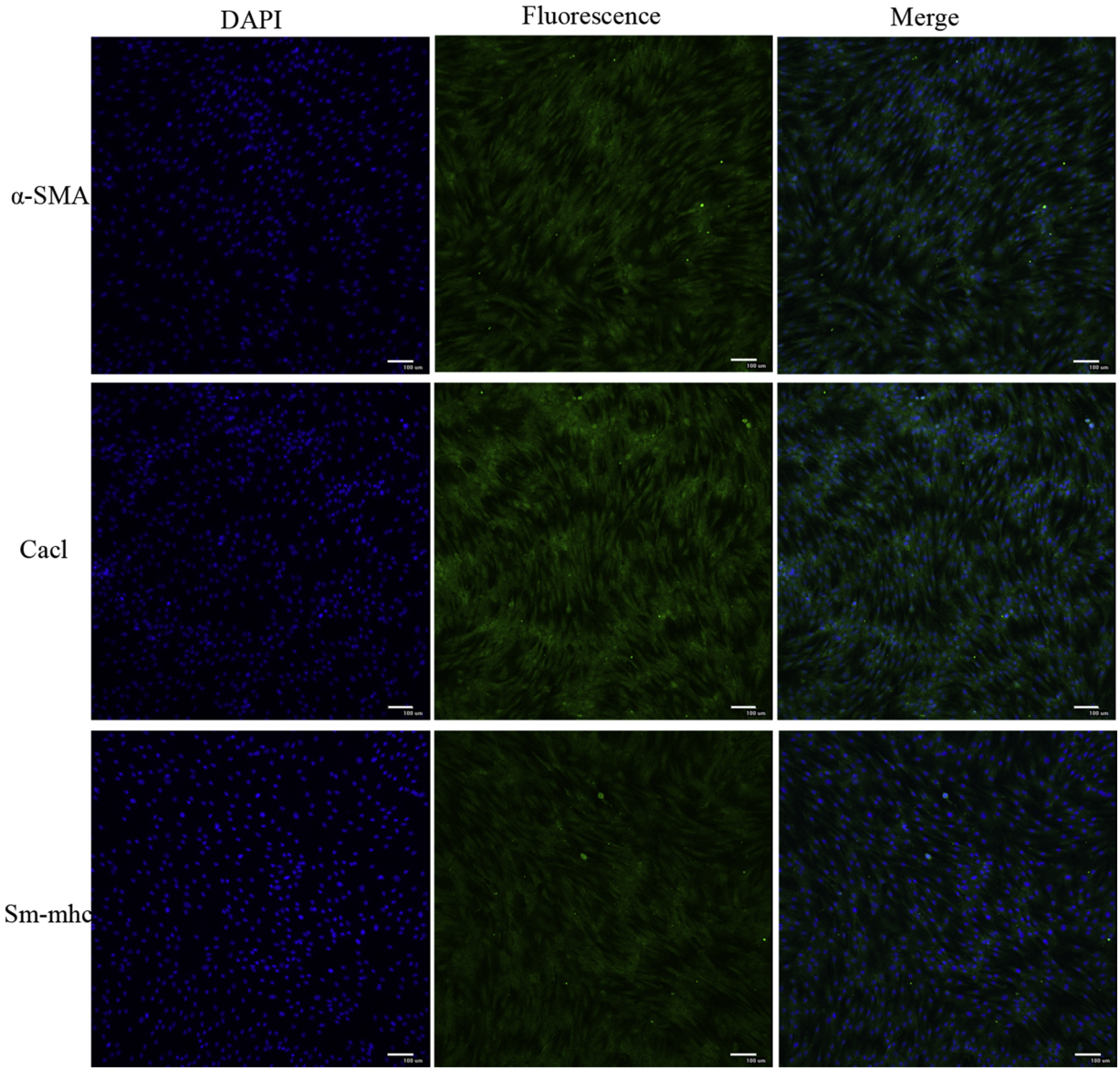

Fig. 8. Smooth muscle cell differentiation of B-PMSCs. After incubation in smooth muscle cell medium for 14 days, the B-PMSCs exhibited obvious morphological variation and immunofluorescence suggested that induced cells expressed specific protein markers α-SMA, calponin-1 and SM-MHC (scale bar = 100 μm).

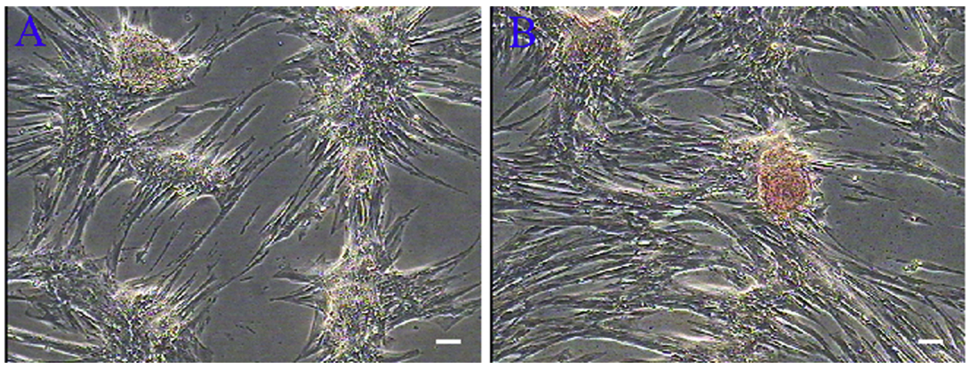

Fig. 9. Insulin-secreting Cell Differentiation of B-PMSCs. **A** islet-like cluster (100×); **B** Dithizone staining (100×). (scale bar = 100 μm).

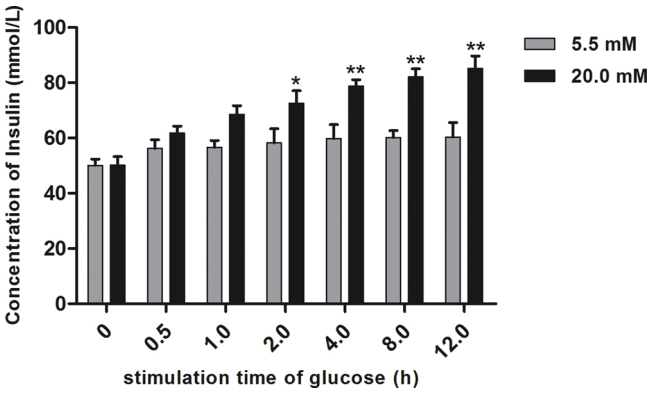

Fig. 10. The B-PMSCs's response to glucose. Bar with * indicates significant differences ($p < 0.05$), while ** indicates significant differences ($p < 0.01$).

Acknowledgments

This research was supported by the Special Fund of Chinese Central Government for Basic Scientific Research Operations in Commonweal Research Institutes (Grant No. 2018-YWF-YTS-9) and National Natural Science Foundation of China (Grant No : 31472099).

References

Badimon, L., Oñate, B., Vilahur, G., 2015. Adipose-derived mesenchymal stem cells and their reparative potential in ischemic heart disease. Rev. Esp. Cardiol. (Engl Ed) 68, 599–611. https://doi.org/10.1016/j.rec.2015.02.025.

Bai, C.Y., Chen, S., Gao, Y.H., Shan, Z., Guan, W.J., Ma, Y.H., 2015. Multi-lineage potential research of bone marrow mesenchymal stem cells from Bama miniature pig. J. Exp. Zool. B Mol. Dev. Evol. 324, 671–685. https://doi.org/10.1002/jez.b.22646.

Boumaza, I., Srinivasan, S., Witt, W.T., Feghali-Bostwick, C., Dai, Y., Garcia-Ocana, A., 2009. Autologous bone marrow-derived rat mesenchymal stem cells promote PDX-1 and insulin expression in the islets, alter T cell cytokine pattern and preserve regulatory T cells in the periphery and induce sustained normoglycemia. J. Autoimmun. 32, 33–42. https://doi.org/10.1016/j.jaut.2008.10.004.

Carlsson, P.O., Schwarcz, E., Korsgren, O., Le Blanc, K., 2015. Preserved β-cell function in type 1 diabetes by mesenchymal stromal cells. Diabetes 64, 587–592. https://doi.org/10.2337/db14-0656.

Damia, E., Chicharro, D., Lopez, S., Cuervo, B., Rubio, M., Sopena, J.J., 2018. Adipose-derived mesenchymal stem cells: are they a good therapeutic strategy for osteoarthritis? Int. J. Mol. Sci. 19. https://doi.org/10.3390/ijms19071926.

De Schauwer, C., Meyer, E., Van de Walle, G.R., Van Soom, A., 2011. Markers of stemness in equine mesenchymal stem cells: a plea for uniformity. Theriogenology 75, 1431–1443. https://doi.org/10.1016/j.theriogenology.2010.11.008.

Gaengel, K., Genove, G., Armulik, A., Betsholtz, C., 2009. Endothelial-mural cell signaling in vascular development and angiogenesis. Arterioscler. Thromb. Vasc. Biol. 29, 630–638. https://doi.org/10.1161/ATVBAHA.107.161521.

Gao, Y.H., Pu, Y., Wang, D., Hou, L.L., Guan, W.J., Ma, Y.H., 2012. Isolation and biological characterization of chicken amnion epithelial cells. Eur. J. Histochem. 29 (56), e33. https://doi.org/10.4081/ejh.2012.e33.

Gao, Y.H., Zhu, Z.Q., Zhao, Y.H., Hua, J.L., Ma, Y.H., Guan, W.J., 2014. Multilineage potential research of bovine amniotic fluid mesenchymal stem cells. Int. J. Mol. Sci. 15, 3698–3710. https://doi.org/10.3390/ijms15033698.

Godfrey, K.J., Mathew, B., Bulman, J.C., Shah, O., Clement, S., Gallicano, G.I., 2012. Stem cell-based treatments for Type 1 diabetes mellitus: bone marrow, embryonic, hepatic, pancreatic and induced pluripotent stem cells. Diabet. Med. 29, 14–23. https://doi.org/10.1111/j.1464-5491.2011.03433.x.

Gopurappilly, R., Bhat, V., Bhonde, R., 2013. Pancreatic tissue resident mesenchymal stromal cell (MSC)-like cells as a source of in vitro islet neogenesis. J. Cell. Biochem. 114, 2240–2247. https://doi.org/10.1002/jcb.24572.

He, X.H., Zhang, S., Lu, tf., Pei, W.H., Zheng, Y.J., Han, X., Guan, W.J., 2018. Characterization of Tibetan Mastiff pancreatic progenitor cells and differentiation into insulin-secreting cells. Int. J. Clin. Exp. Med. 11, 1632–1643 www.ijcem.com /ISSN:1940-5901/IJCEM0061374.

Jiao, Y.Q., Yi, Z.W., He, X.J., Liu, X.H., He, Q.N., Huang, D.L., 2011. Does injection of metanephric mesenchymal cells improve renal function in rats? Saudi J. Kidney Dis. Transpl. 22, 501–510 PMID: 21566308.

Lin, C.H., Lilly, B., 2014. Endothelial cells direct mesenchymal stem cells toward a smooth muscle cell fate. Stem Cells Dev. 23, 2581–2590. https://doi.org/10.1089/scd.2014.0163.

Little, M.H., 2006. Regrow or repair: potential regenerative therapies for the kidney. J. Am. Soc. Nephrol. 17, 2390–2401. https://doi.org/10.1681/ASN.2006030218.

Ma, C.Y., Guo, Y.H., Liu, H., Wang, K.F., Yang, J.J., Li, X.C., 2016. Isolation and Biological Characterization of a novel type of Pulmonary Mesenchymal Stem Cells derived from Wuzhishan Miniature pig embryo. Cell Biol. Int. 40, 1041–1049. https://doi.org/10.1002/cbin.10643.

Marion, N.W., Mao, J.J., 2006. Mesenchymal stem cells and tissue engineering. Methods Enzymol 420, 339–361. https://doi.org/10.1016/S0076-6879(06)20016-8.

Mathew, S.A., Bhonde, R., 2017. Mesenchymal stromal cells isolated from gestationally diabetic human placenta exhibit insulin resistance, decreased clonogenicity and angiogenesis. Placenta 59, 1–8. https://doi.org/10.1016/j.placenta.2017.09. 002.

Mendes, F.D., Ribeiro, P.D.C., Oliveira, L.F., de Paula, D.R.M., Capuano, V., de Assunção, T.S.F., 2018. Therapy with mesenchymal stem cells in parkinson disease: history and perspectives. Neurologist 23, 141–147. https://doi.org/10.1097/NRL.0000000000000188.

Murai, N., Ohtaki, H., Watanabe, J., Xu, Z., Sasaki, S., Yagura, K., 2017. Intrapancreatic injection of human bone marrow-derived mesenchymal stem/stromal cells alleviates hyperglycemia and modulates the macrophage state in streptozotocin-induced type 1 diabetic mice. PLoS One 12, e0186637. https://doi.org/10.1371/journal.pone.0186637.

Okura, H., Komoda, H., Fumimoto, Y., Lee, C.M., Nishida, T., Sawa, Y., 2009. Transdifferentiation of human adipose tissuederived stromal cells into insulin-producing clusters. J. Artif. Organs 12, 123–130. https://doi.org/10.1007/s10047-009-0455-6.

Otonkoski, T., Gao, R., Lundin, K., 2005. Stem cells in the treatment of diabetes. Ann. Med. 37, 513–520. https://doi.org/10.1080/07853890500300279.

Phadnis, S.M., Joglekar, M.V., Dalvi, M.P., Muthyala, S., Nair, P.D., Ghaskadbi, S.M., 2011. Human bone marrow-derived mesenchymal cells differentiate and mature into endocrine pancreatic lineage in vivo. Cytotherapy 13, 279–293. https://doi.org/10.3109/14653249.2010.523108.

Prockop, D.J., Olson, S.D., 2007. Clinical trials with adult stem/progenitor cells for tissue repair: let's not overlook some essential precautions. Blood 109, 3147–3151. https://doi.org/10.1182/blood-2006-03-013433.

Sagrinati, C., Ronconi, E., Lazzeri, E., Lasagni, L., Romagnani, P., 2008. Stem-cell approaches for kidney repair: choosing the right cells. Trends Mol. Med. 14, 277–285. https://doi.org/10.1016/j.molmed.2008.05.005.

Seeberger, K.L., Dufour, J.M., Shapiro, A.M., Lakey, J.R., Rajotte, R.V., Korbutt, G.S., 2006. Expansion of mesenchymal stem cells from human pancreatic ductal epithelium. Lab. Investig. 86, 141–153. https://doi.org/10.1038/labinvest.3700377.

Shapiro, A.M., Ricordi, C., Hering, B.J., Auchincloss, H., Lindblad, R., Robertson, R.P., 2006. International trial of the Edmonton protocol for islet transplantation. N. Engl. J. Med. 355, 1318–1330. https://doi.org/10.1056/NEJMoa061267.

Silva, A.C., Percegona, L.S., França, A.L., Dos Santos, T.M., Perini, C.C., González, P., 2012. Expression of pancreatic endocrine markers by mesenchymal stem cells from human adipose tissue. Transplant. Proc. 44, 2495–2496. https://doi.org/10.1016/j.transproceed.2012.07.036.

Uccelli, A., Prockop, D.J., 2010. Why should mesenchymal stem cells (MSCs) cure autoimmune diseases? Curr. Opin. Immunol. 22, 768–774. https://doi.org/10.1016/j.coi. 2010.10.012.

Wang, H.W., Lin, L.M., He, H.Y., You, F., Li, W.Z., Huang, T.H., 2011. Human umbilical cord mesenchymal stem cells derived from Wharton's jelly differentiate into insulin-producing cells in vitro. Chin. Med. J. 124, 1534–1539 PMID: 21740812.

Wen, H.B., Tian, X.Z., Wu, X.L., Zheng, Y.J., Ji, H.D., Sun, Y.Z., Guan, W.J., 2018. Multilineage potential research on metanephric mesenchymal stem cells of bama miniature pig. J Biomater Tiss. Eng Epub ahead of print.

Williams, A.R., Hare, J.M., 2011. Mesenchymal stem cells: biology, pathophysiology, translational findings, and therapeutic implications for cardiac disease. Circ. Res. 109, 923–940. https://doi.org/10.1161/CIRCRESAHA.111.243147.

Yeung, T.Y., Seeberger, K.L., Kin, T., Adesida, A., Jomha, N., Shapiro, A.M., 2012. Human mesenchymal stem cells protect human islets from pro-inflammatory cytokines. PLoS One 7, e38189. https://doi.org/10.1371/journal.pone.0038189.